2019

Parametric characterization of penumbra reduction for aperture-collimated pencil beam scanning (PBS) proton therapy

Dominic Maes
Seattle Cancer Care Alliance Proton Therapy Center, dm113@uowmail.edu.au

Rajesh Regmi
Seattle Cancer Care Alliance Proton Therapy Center

Phillip Taddei
University of Washington

Charles Bloch
University of Washington

Steven Bowen
University of Washington

See next page for additional authors

Parametric characterization of penumbra reduction for aperture-collimated pencil beam scanning (PBS) proton therapy

Abstract

Recently, a commercial treatment planning system (TPS) has implemented aperture collimators for PBS dose calculations which can serve to reduce lateral penumbra. This study characterized the variation in magnitude of lateral penumbra for collimated and un-collimated PBS fields versus the parameters of air gap, depth, and range shifter thickness. Comparisons were performed in a homogenous geometry between measured data and calculations made by a commercial TPS. Beam-specific target volumes were generated for collimated and un-collimated PBS fields and optimized for various range shifter thicknesses and air gaps. Lateral penumbra (80%-20% distance) was measured across each target volume to characterize penumbra variation with depth and air gap. An analytic equation was introduced to predict the reduction in lateral penumbra between un-collimated and collimated PBS treatments. Calculated penumbra values increased with depth across all combinations of range shifters for a constant air gap. At 2 cm depth, the reductions in penumbra due to the aperture were 2.7 mm, 3.7 mm and 4.2 mm when using range shifter thicknesses of 0 cm, 4.0 cm and 7.5 cm, respectively. At a depth of approximately 20 cm and air gap of 5 cm, differences between penumbras of collimated and un-collimated beams were less than 1 mm. Penumbra reductions for the collimated beams were largest at small air gaps. All TPS-calculated penumbra values derived in this study were within 1 mm of film measurement values. Finally, the analytic equation was tested using a clinical CT scan, and we found good dosimetric agreement between the model predictions and the result calculated by the TPS. In conclusion, application of collimators to PBS fields can sharpen penumbra by several mm and are most beneficial for shallow targets. Furthermore, measurements indicate that the dose calculation accuracy in the penumbra region of PBS-collimated fields is adequate for clinical use.

Disciplines

Engineering | Science and Technology Studies

Publication Details

Maes, D., Regmi, R., Taddei, P., Bloch, C., Bowen, S., Nevitt, A., Leuro, E., Wong, T., Rozenfeld, A. & Saini, J. (2019). Parametric characterization of penumbra reduction for aperture-collimated pencil beam scanning (PBS) proton therapy. Biomedical Physics and Engineering Express, 5 (3), 035002-1-035002-10.

Authors

Dominic Maes, Rajesh Regmi, Phillip Taddei, Charles Bloch, Steven Bowen, Alexander Nevitt, Erick Leuro, Tony Wong, Anatoly B. Rosenfeld, and Jatinder Saini

Parametric characterization of penumbra reduction for aperture-collimated pencil beam scanning (PBS) proton therapy

Dominic Maes[1], Rajesh Regmi[1], Phillip Taddei[2], Charles Bloch[2], Steven Bowen[2], Alexander Nevitt[1], Erick Leuro[1], Tony Wong[1], Anatoly Rosenfeld[3], Jatinder Saini[1]

[1] Seattle Cancer Care Alliance Proton Therapy Center, 1570 N 115th St., Seattle, WA 98133, United States of America
[2] Departments of Radiation Oncology and Radiology, University of Washington School of Medicine, 1959 NE Pacific St., Seattle, WA 98195, United States of America
[3] Centre for Medical Radiation Physics, University of Wollongong, Wollongong, Australia

E-mail: Dominic.Maes@seattleprotons.org

Keywords: Proton therapy, pencil beam scanning, penumbra

Abstract

Recently, a commercial treatment planning system (TPS) has implemented aperture collimators for PBS dose calculations which can serve to reduce lateral penumbra. This study characterized the variation in magnitude of lateral penumbra for collimated and un-collimated PBS fields versus the parameters of air gap, depth, and range shifter thickness. Comparisons were performed in a homogenous geometry between measured data and calculations made by a commercial TPS. Beam-specific target volumes were generated for collimated and un-collimated PBS fields and optimized for various range shifter thicknesses and air gaps. Lateral penumbra (80%-20% distance) was measured across each target volume to characterize penumbra variation with depth and air gap. An analytic equation was introduced to predict the reduction in lateral penumbra between un-collimated and collimated PBS treatments. Calculated penumbra values increased with depth across all combinations of range shifters for a constant air gap. At 2 cm depth, the reductions in penumbra due to the aperture were 2.7 mm, 3.7 mm and 4.2 mm when using range shifter thicknesses of 0 cm, 4.0 cm and 7.5 cm, respectively. At a depth of approximately 20 cm and air gap of 5 cm, differences between penumbras of collimated and un-collimated beams were less than 1 mm. Penumbra reductions for the collimated beams were largest at small air gaps. All TPS-calculated penumbra values derived in this study were within 1 mm of film measurement values. Finally, the analytic equation was tested using a clinical CT scan, and we found good dosimetric agreement between the model predictions and the result calculated by the TPS. In conclusion, application of collimators to PBS fields can sharpen penumbra by several mm and are most beneficial for shallow targets. Furthermore, measurements indicate that the dose calculation accuracy in the penumbra region of PBS-collimated fields is adequate for clinical use.

1. Introduction

PBS of proton beams allows for highly conformal treatment deliveries, minimizing dose to surrounding tissue (Saini et al., 2017, Liu and Chang, 2011). This is accomplished by careful placement of spots tightly around the target volume in a way that limits dose to healthy tissue (Liu and Chang, 2011). However, other proton beam delivery techniques, such as passive scattering, employ aperture collimation that allows for sharper lateral penumbra than PBS without apertures. Recently, a widely-used commercial treatment planning system (TPS) (RayStation, version 6, RaySearch Laboratories, Stockholm, Sweden) has coupled the strengths of each delivery technique by adding the application of apertures to PBS fields (Saini et al., 2017, Saini et al., 2016, Baumer et al., 2017). While PBS delivery has traditionally been delivered without the application of apertures, the use of aperture collimation can reduce lateral penumbra and, therefore, minimize dose to critical organs at risk for certain disease sites (Charlwood et al., 2016).

Multiple studies have been conducted investigating the use of apertures in PBS proton beam delivery (Rana et al., 2013, Charlwood et al., 2016, Gottschalk, 2011, Urie et al., 1986, Safai et al., 2008, Winterhalter et al., 2017, Titt et al., 2010, Baumer et al., 2018). For example, Charlwood et al. performed Monte Carlo (MC) simulations of a PBS nozzle and characterized lateral penumbra as a function of depth for varying energies and found adding collimation to a PBS beam can sharpen penumbra by 2 – 4 mm depending on depth (Charlwood et al., 2016). Safai *et al.* compared the lateral penumbra between a collimated proton double-scattered (DS) beam and un-collimated PBS beam and found that the penumbra of a pencil beam at shallow depth is larger than the penumbra of a collimated DS beam, but better at larger depths (Safai et al., 2008). Winterhalter *et al.* characterized the lateral penumbra of PBS beams with and without aperture collimation using the TOPAS (Perl et al., 2012) MC toolkit (Winterhalter et al., 2017). Finally, Baumer et al. demonstrated that superior lateral penumbra reduction can be achieved when the aperture is mounted downstream of the range shifter (Baumer et al., 2018). In this same study Baumer et al. validated the lateral penumbra calculated with the Raystation Monte Carlo algorithm against measurements carried out an ionization chamber array and scintillator detector and found excellent agreement within 0.5 mm (Baumer et al., 2018).

With the exception of Baumer et al. these studies did not validate the lateral penumbra reduction of aperture-collimated PBS beams using a clinically commissioned TPS, a process that is required for clinical implementation of apertures in PBS proton therapy. While Baumer et al. performed validation of Raystation for lateral penumbra calculation of collimated PBS fields for varying energy and depths, there was however no mention of the accuracy of penumbra calculation across varying airgaps or range shifter thickness both of which can significantly affect PBS penumbra. Characterization and validation of the Raystation TPS for collimated PBS fields across all relevant planning parameters which can affect lateral penumbra is needed for clinical commissioning of aperture-collimated PBS beam delivery.

The aim of this study was twofold. The first aim was to validate the Raystation TPS MC dose calculation of lateral penumbra of aperture-collimated PBS beams against film for all relevant parameters that affect lateral penumbra including depth, air gap and range shifter thickness. The second aim of this work was to comprehensively characterize the reduction in lateral penumbra between un-collimated and collimated PBS fields for varying values of these parameters. We accomplished these aims by optimizing PBS beams using various combinations of planning parameters in a homogenous geometry and validating the TPS-calculated penumbra values against film measurements.

2. Methods and Materials

2.1. Proton beam delivery system

Measurements for this study were carried out on a fixed PBS beam line that delivers fields at 90 degrees. Our clinic is equipped with a proton delivery system (Proteus PLUS, Ion Beam Applications, Louvain-La-Neuve, Belgium) with a cyclotron that accelerates proton beams with a fixed energy of 230 MeV. An energy degrader is applied to modulate this energy through a continuous energy range of 98.5 MeV to 228.5 MeV. In-air proton beams spots are Gaussian in shape with sigma values at isocenter ranging approximately from 3.2 mm to 7.3 mm for 228.5 MeV and 95.5 MeV beam spots respectively. For PBS treatment fields delivered on the fixed beam-line, our system is clinically commissioned to deliver a maximum field size of 40 cm x 30 cm with a continuous range in water from 7.5 cm to 32.5 cm. For shallow targets, i.e., at water-equivalent depths of less than 7.5 cm, acrylic range shifters are added to the end of the treatment unit for additional modulation. Our TPS has been commissioned to support the use of either a 4.0 cm or 7.5 cm water equivalent thickness range shifter (Saini et al., 2016).

2.2. Treatment Planning Optimization Parameters

Treatment planning of PBS beam delivery was performed in RayStation v6.0. The TPS supports two dose calculation algorithms: Pencil Beam dose engine (version 4.1) as well as the Monte Carlo dose engine (version 4.0) (RS-MC) (Saini et al., 2017, Hong et al., 1996, Baumer et al., 2017, Laboratories, 2017).

Each PBS treatment field in this study was optimized using an inverse treatment planning method. Specifically, absorbed dose was calculated using RS-MC with a 2 mm isotropic calculation grid. Each field was optimized using 10,000 ions/spot for 200 iterations. Plan optimization objectives were set to deliver a minimum dose of 30.0 Gy (RBE) in 10 fractions (3 Gy (RBE) per fraction) in the target volume. The target volume was consistent between plans, consisting of a rectangular cuboid with dimensions of 10 cm x 10 cm at isocenter and varying length along the beam axis. A maximum dose objective of 30.9 Gy (RBE) (i.e. 103%) was placed on the external volume to control hotspots and ensure dose uniformity within the target volume. Each plan consisted of a single beam incident enface on a phantom optimized to deliver uniform dose across the target. Additional beam computation settings used for optimization included an initial spot placement target margin of 0.6 cm around each target as well as variable energy layer and inter spot-spacing parameters relative to the Bragg peak width and spot size, respectively (energy spacing = 1, spot spacing = 0.5). Following the completion of 200 iterations a final dose calculation was carried out using RS-MC with a statistical uncertainty of 0.5%.

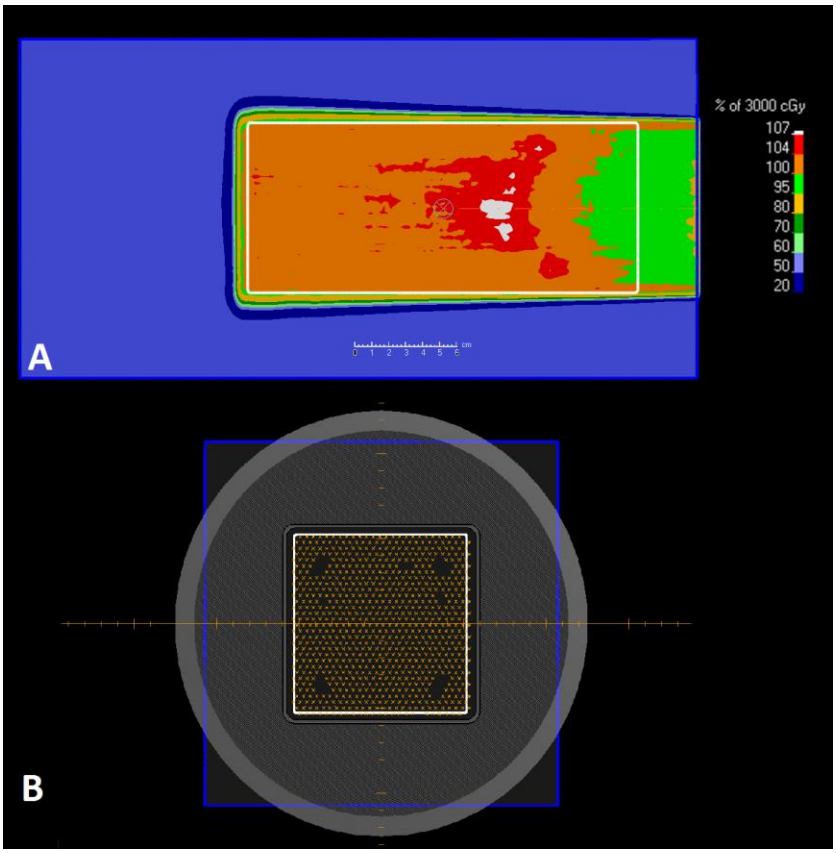

Figure 1: (A) Lateral dose color wash profile of a single beam optimized to deliver uniform dose the target (white contour) in a water phantom (blue volume) using a collimated PBS beam and 4.0 cm range compensator. (B) Beams eye view showing spot placement around the target for the same collimated PBS beam.

Each treatment field was copied and brass apertures of 6.5 cm thickness were then applied in the TPS. These fields were also optimized using RS-MC, with a 0.6 cm aperture target margin and 0.5% uncertainty.

2.3. Investigation methodology

2.3.1. Variation of lateral penumbra with depth

First, the relationship between PBS penumbra and depth was analyzed in the following manner: Three separate treatment fields were optimized independently such that 95% of the target volume was covered by 95% of the prescription dose (i.e. D95%=30 Gy (RBE)). These three fields corresponded to three different range shifters: 0 cm (RS0), 4.0cm (RS40), and 7.5cm (RS75). The physical thicknesses of the acrylic range shifters used at our clinic are 3.5 cm for RS40 and 6.5 cm for RS75.

Beam specific target volumes of field size 10x10 cm were created such that the optimized plan would have the maximum possible range and width of spread out Bragg peak (SOBP) for each range shifter. The resulting plans were (i) range 31 cm, SOBP width 23 cm for RS0, (ii) range 27 cm, SOBP width 23 cm for RS40, and (iii) range 23.5 cm, SOBP width 23 cm for RS75. Following optimization, dose files were exported and analyzed in DoseLab (version 6.60, Mobius Medical Systems LP, Bellaire, TX, USA). Lateral

penumbra (80%-20% distance) was recorded at 2 cm intervals in depth along each target volume without the use of an aperture.

Next, brass aperture collimation was applied in the TPS and each field was re-optimized with RS-MC to ensure original target dose coverage (D95%=95%). Lateral penumbra of aperture-collimated fields was then re-analyzed at 2 cm intervals along each target volume. For fields using a range shifter, a 5 cm airgap was applied. In this study air gap is defined as the distance between the downstream range shifter surface and upstream phantom surface. In this configuration, the distance from isocenter to the downstream surface of RS40 and RS75 was 20 cm. In the TPS, apertures are placed directly upstream from the range shifter. The corresponding distance from isocenter to the downstream surface of the brass apertures was 20cm, 23.5cm and 26.5cm when using RS0, RS40 and RS75 respectively.

2.3.2. Film Measurements

TPS data were compared against film to validate RS-MC penumbra calculation of aperture-collimated PBS beams. First, all aperture-collimated PBS fields were transferred to the Mosaiq™ (Elekta, Sweden) radiation oncology information system. TPS measurement conditions were mimicked by placing Gafchromic EBT3 (Ashland, NJ) films between slabs of solid water. The solid water slabs were set on the treatment couch with each film placed at specified depths. The treatment couch was then positioned to align the solid water to treatment isocenter before beam delivery. The irradiated films were scanned 24 hours after exposure using a flatbed scanner (Epson Expression 11000XL, Epson America Inc., CA) and each pixel value was converted to optical density (OD) using the red channel. A non-irradiated film was also scanned in the same set up and subtracted from the irradiated films to account for background. Finally, the OD files were converted to absolute dose value through a dose-OD calibration curve. Scanner resolution was set at 72 pixels per inch in the landscape orientation. Digitized films were exported to the DoseLab software and lateral penumbra values measured with film were analyzed and recorded.

2.3.3. Variation of lateral penumbra with air gap

Next, the relationship between PBS penumbra and air gap between the range shifter and patient surface was analyzed. Six beams of varying air gaps ranging from 5 - 30 cm in 5 cm increments were generated using RS40 and RS75. Note that use of RS0 was excluded because the air gap is undefined in this case. For each beam, the target volume consisted of a 10x10x10 cm^3 cube centered at depth of 15 cm inside a homogenous water volume resulting in a beam of range 20 cm with SOBP width of 10 cm. Following optimization, dose files were exported and lateral penumbra was evaluated at depths of 7, 11, 15 and 19 cm using DoseLab. Next, brass aperture collimators were applied in the TPS and each field was recalculated with RS-MC. The resulting lateral penumbra values were analyzed at the same intervals as in the non-aperture case.

2.3.4. Dosimetric comparison using a patient CT

In this example, three un-collimated PBS fields were optimized in Raystation using the single field uniform dose technique to deliver 5040 cGy (RBE) in a lesion in the pineal region of the brain in 28 fractions (180 cGy (RBE) per fraction). The field arrangement in this example included a vertex as well as right and left superior oblique beams. For this treatment plan, an air gap of 5 cm was used along with the RS40 range shifter for all three fields. Optimization was performed with RS-MC using 10,000 ions/spot. Following optimization a final RS-MC dose calculation was performed using an uncertainty setting of 1%. Additional

TPS settings for this plan included a spot spacing of 0.7 cm, energy layer spacing of 0.8 cm and spot placement target margin of 0.7 cm. Next, brass apertures were applied to each field using an aperture target margin of 0.7 cm. Treatment fields were then reset and re-optimized using the same settings and optimization objectives. The resulting isodose distributions and DVH data were analyzed.

3. Results

3.1. Lateral Penumbra vs. Depth

Application of an aperture to PBS fields resulted in a reduction in lateral penumbra for all analyzed depths across all three range shifter thicknesses.

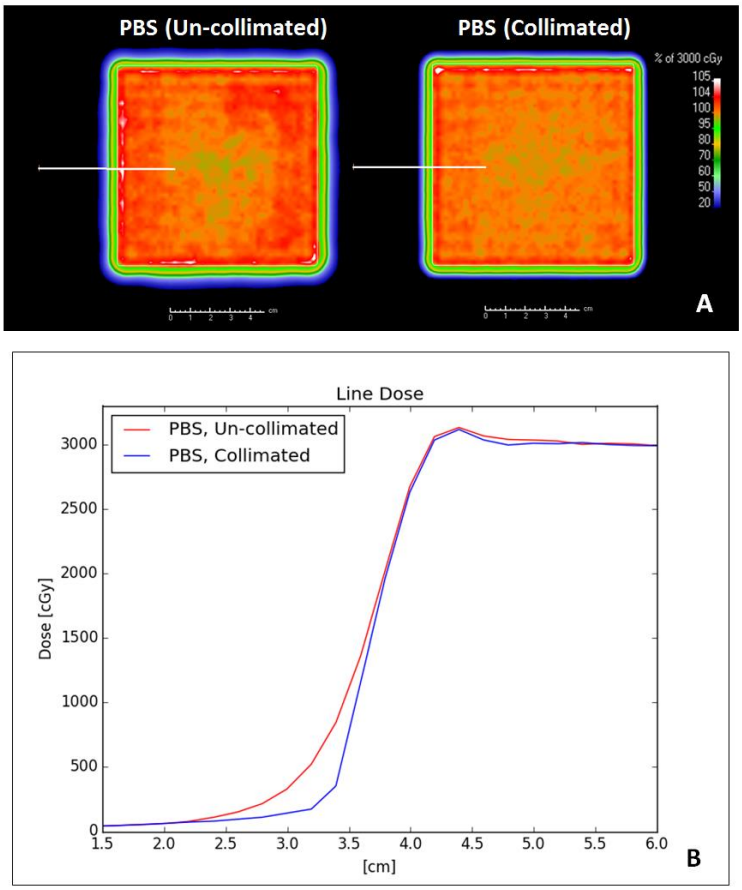

Figure 2: (A): TPS-calculated two-dimensional absorbed dose distributions for a PBS field with and without aperture collimation in a homogenous water phantom at 9 cm depth using a 0 cm range shifter and (B) one-dimensional dose profiles calculated by the TPS illustrating the lateral penumbra for a collimated (blue line) and un-collimated (red line) PBS field. The white line in (A) indicates the location of the profile shown in (B).

Reduction in PBS lateral penumbra due to collimation was most significant at shallow depths and decreased with depth. Figure 2 illustrates the lateral penumbra for a PBS field in homogenous geometry with and without collimation as calculated by the TPS. Figure 2 also illustrates the lateral penumbra for a PBS field

in homogenous geometry as calculated by the TPS for one beam setting. The reduction in penumbra with collimation versus without collimation is clearly observed. Figure 3 plots the TPS-calculated penumbra as a function of depth for all three range shifters (RS0, RS40, and RS75). For each range shifter, lateral penumbra is reported for the collimated field as calculated by RS-MC, the un-collimated field as calculated by RS-MC, and the collimated field as measured by film. All film measured values of lateral penumbra matched RS-MC within +/- 1 mm (maximum variation = 0.7 mm, mean variation = 0.3 mm, standard deviation = 0.2 mm).

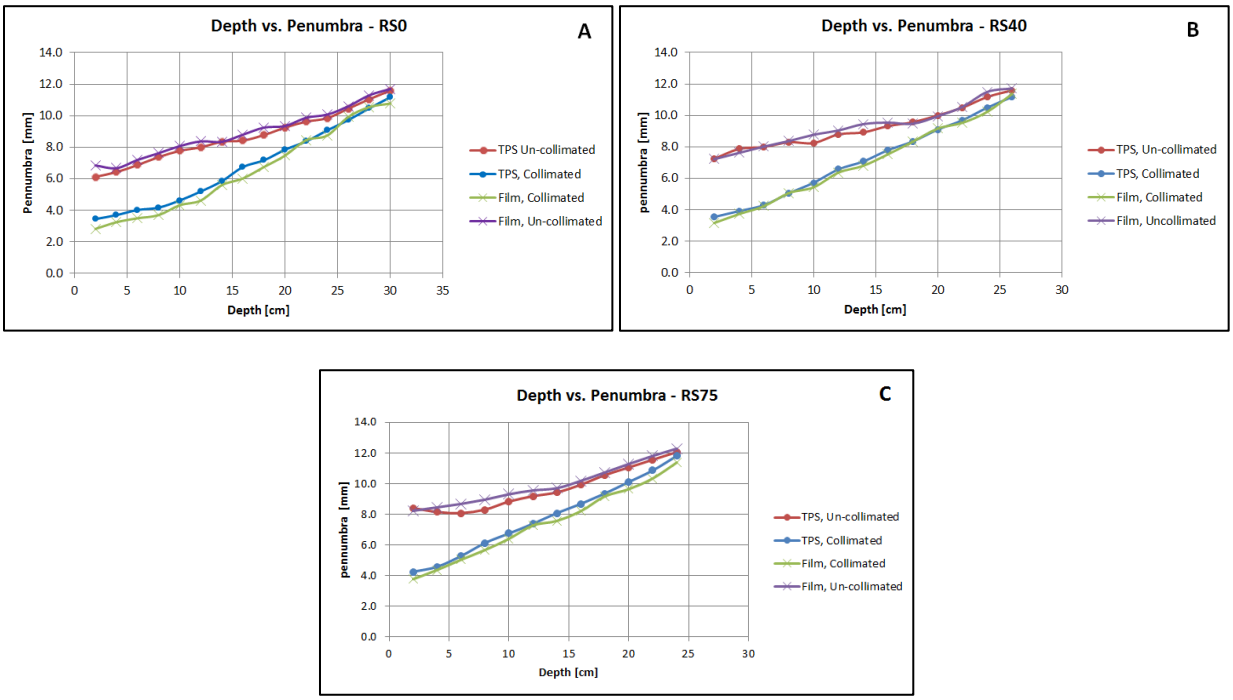

Figure 3: TPS-calculated and measured penumbra showing the comparison of lateral penumbra with and without the use of an aperture for three different beams with varying range shifter thickness range and SOBP width. (A): range 31 cm, SOBP width 23 cm, RS0. (B): range 27 cm, SOBP width 23 cm, RS40. (C): range 23.5 cm, SOBP width 23 cm, RS75.

The magnitude of lateral penumbra increased approximately linearly with depth for all three range shifters with and without aperture collimation. With varying range shifter thickness and same SOBP width, we observed excellent agreement between penumbra values calculated with RS-MC and those measured with film.

A scatter plot of lateral penumbra reduction vs. depth is presented in Figure 4. Linear regression curves are overlaid onto the scatter plots to illustrate the trend and slope of penumbra variation with depth.

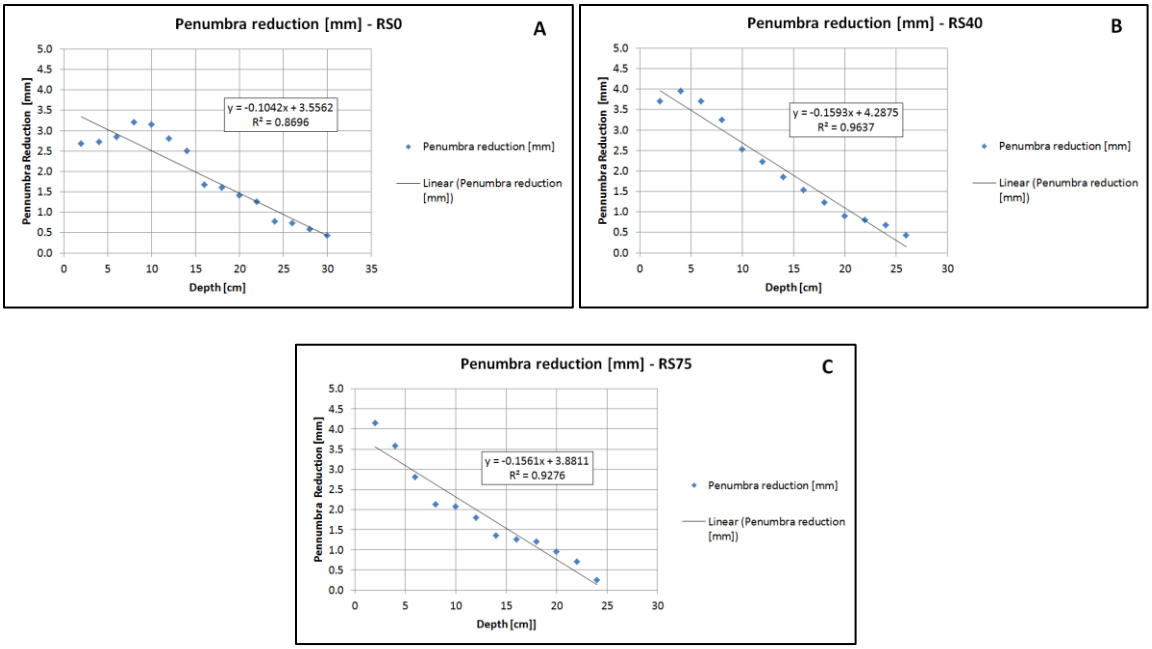

Figure 4: Comparison of TPS calculated lateral penumbra reduction with and without aperture collimation for the three different range shifter thicknesses shown in Figure 2.

The linear slope of penumbra reduction per unit change in depth is -0.10 mm/cm for RS0 and -0.16 mm/cm for RS40 and RS75. At 2 cm (i.e. the shallowest depth), penumbra reduction was 2.7 mm, 3.7 mm and 4.2 mm for RS0, RS45 and RS75 respectively. Penumbra reduction was reduced to 1 mm at a depth of approximately 23 cm for RS0 and 20 cm for RS40 and RS75.

3.2. Lateral Penumbra vs. Air gap

Figure 5 shows the lateral penumbra values for all air gaps (5 -30 cm in 5 cm increments) calculated by RS-MC at four depths for the 4 cm and 7.5 cm range shifters.

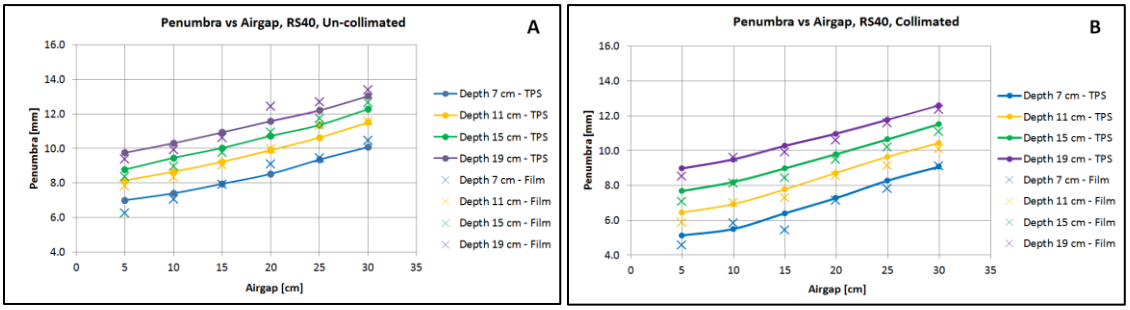

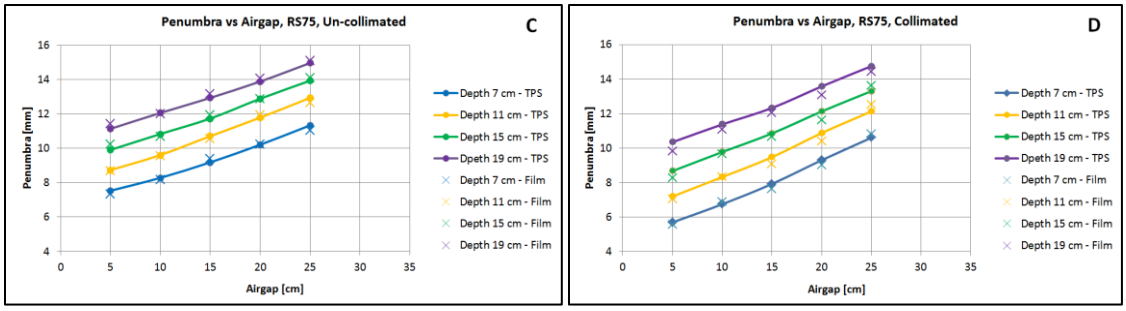

Figure 5: Variation of TPS-calculated lateral penumbra at multiple depths as a function of air gap for RS40 - un-collimated (A), RS40 - collimated (B), RS75 – un-collimated (C) and RS75 – Collimated (D).

Lateral penumbra increased approximately linearly with both depth and air gap for both RS40 and RS75. For RS40 without collimation, the lateral penumbra increased from 7 mm (depth 7 cm, air gap 5 cm) to 13 mm (depth 19 cm, air gap 30 cm). With collimation, the lateral penumbra increased from 5.1 mm (depth 7 cm, air gap 5 cm) to 12.6 mm (depth 19 cm, air gap 30 cm). For RS75 without collimation, the lateral penumbra increased from 7.5 mm (depth 7 cm, air gap 5 cm) to 14.9 mm (depth 19 cm, air gap 30 cm). With collimation, the lateral penumbra increased from 5.7 mm (depth 7 cm, air gap 5 cm) to 14.8 mm (depth 19 cm, air gap 30 cm). All TPS-calculated lateral penumbra values of PBS-collimated fields agreed with film measurements within +/- 1 mm (max variation = 0.9 mm, mean variation = 0.3 mm, standard deviation = 0.2) across all combinations of air gap and depth.

Applying a 2nd order polynomial surface fit to the penumbra reduction, *PR*, as a function of depth and airgap results in the following relationship:

$$PR = C_1 + C_2 AG + C_3 d + C_4 (AG)(d) + C_5 AG^2 + C_6 d^2 \quad (1)$$

where *d* is the water phantom depth, *AG* is the airgap between the phantom and range shifter. The fitting parameters, $C_1 - C_6$, for Equation 1 are shown in table below for RS40 and RS75.

	RS40	***RS75***
$\boldsymbol{C_1}$	2.39	2.07
$\boldsymbol{C_2}$	$-5.53\ x\ 10^{-2}$	$-6.95\ x\ 10^{-2}$
$\boldsymbol{C_3}$	$-4.49\ x\ 10^{-3}$	$2.73\ x\ 10^{-2}$
$\boldsymbol{C_4}$	$2.16\ x\ 10^{-3}$	$2.17\ x\ 10^{-3}$
$\boldsymbol{C_5}$	$-1.07\ x\ 10^{-5}$	$9.29\ x\ 10^{-5}$
$\boldsymbol{C_6}$	$-4.30\ x\ 10^{-3}$	$-4.66\ x\ 10^{-3}$

Table 1: Fitting parameters for a 2nd order polynomial surface fit of penumbra reduction as a function of depth and airgap.

Figure 6 shows 2D contour plots of this surface fit generated from the RS40 and RS75 data illustrating penumbra reduction as a function of air gap and depth.

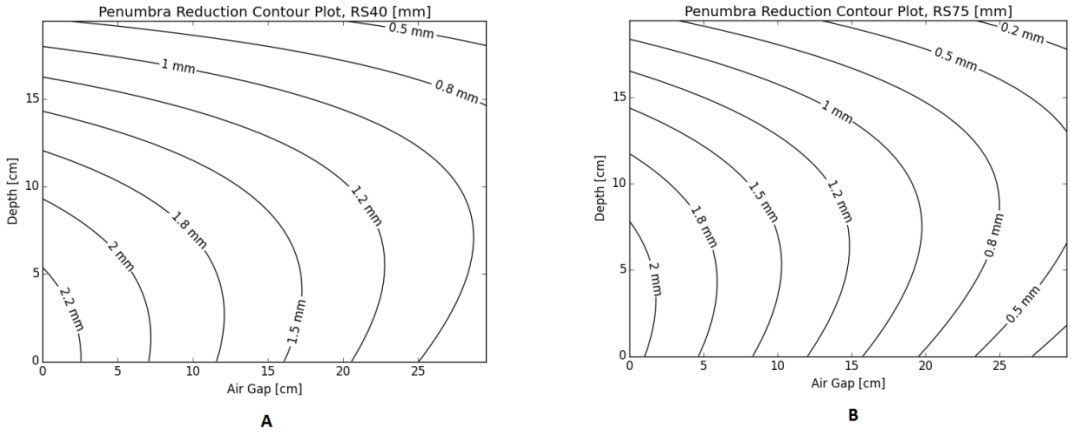

Figure 6: 2D contour plot illustrating TPS-calculated lateral penumbra reduction as function of airgap and depth for RS40 (A) and RS75 (B)

Penumbra reduction was largest at shallow depths and small air gaps when using both RS40 and RS75. Penumbra reduction decreased as both the depth and air gap are increased.

3.3. Clinical Patient Example

A clinical example patient is presented here to compare penumbra reduction between collimated and un-collimated PBS treatment fields. The field arrangement for this treatment plan is shown in Figure 7.

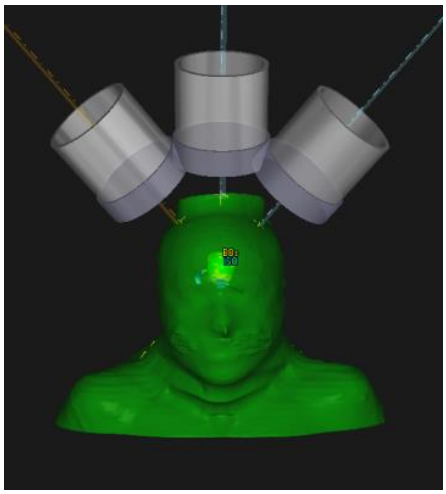

Figure 7: 3D view of the beam arrangement used in the clinical example.

Figure 8 shows axial dose distributions of the un-collimated PBS plan (8A), collimated PBS plan (8B), dose difference (8C) and line dose profile across the two treatment plans (8D).

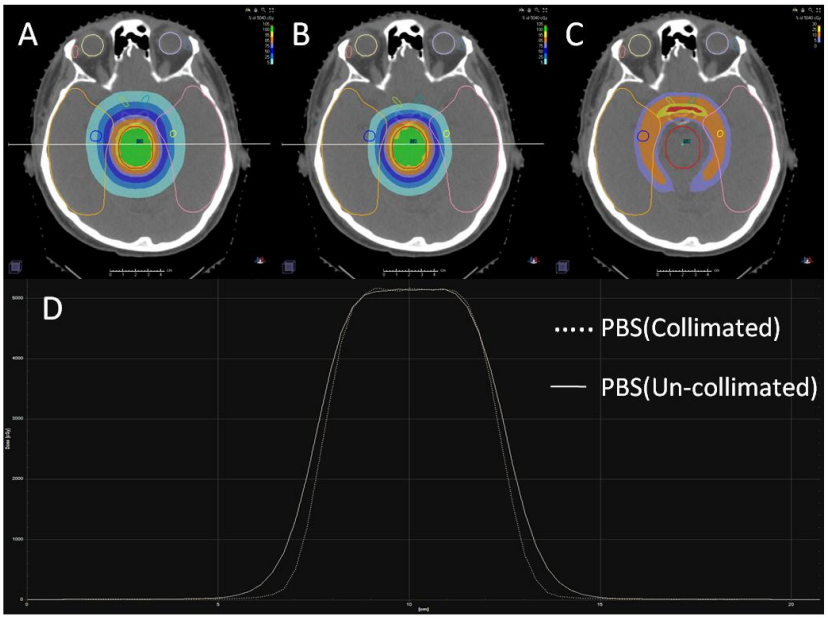

Figure 8: Axial dose distributions for the un-collimated PBS plan (A), collimated PBS plan (B) dose difference (C) and line dose profile across the two treatment plans (D).

The line dose profiles in Figure 8D were analyzed in Doselab and had an average (right-left) lateral penumbra of 1.25 cm for the un-collimated PBS plan and 1.02 cm for the aperture-collimated plan. The corresponding average reduction in penumbra along the right and left side of the target in the axial view as shown in Figure 8 is therefore 2.3 mm. This value is in good agreement with Equation 1 which yields a lateral penumbra calculation of 1.9 mm when using the fitting parameters shown in Table 1, an airgap of 5 cm and depth of 6 cm which is the approximate depth the target (red contour) shown in Figure 8.

Figure 9 shows the corresponding DVH for the collimated and un-collimated PBS plans shown in Figure 8.

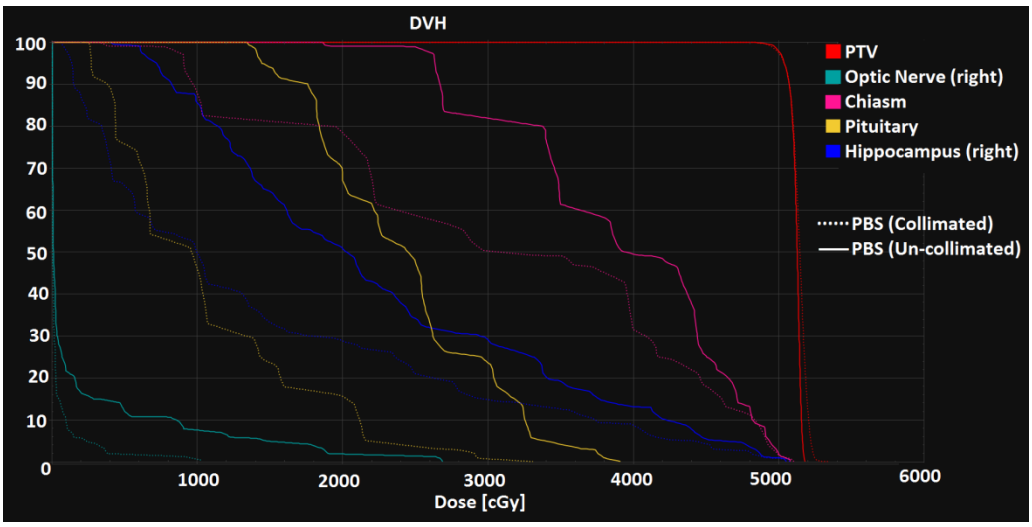

Figure 9: Dose volume histogram showing dose to the target and multiple nearby OARs for PBS plans optimized with and without aperture collimation.

As can be seen in Figure 9, target dose is maintained while dose to several nearby OARs is reduced. Figure 10 shows the corresponding dose statistics for the PTV and multiple affected OARs.

Plan	ROI	ROI vol. [cm3]	Dose [cGy]		
			D99	Average	D1
PBS - Collimated	Chaism	0.29	629	3063	5050
PBS - Un-collimated	Chaism	0.29	2124	3922	5049
PBS - Collimated	Hippocampus R	1.27	85	1440	4908
PBS - Un-collimated	Hippocampus R	1.27	608	2261	4924
PBS - Collimated	Optic Nerve L	0.51	4	47	945
PBS - Un-collimated	Optic Nerve L	0.51	5	209	2647
PBS - Collimated	Optic Nerve R	0.51	2	54	947
PBS - Un-collimated	Optic Nerve R	0.51	4	239	2675
PBS - Collimated	Pituitary	0.49	265	1047	2926
PBS - Un-collimated	Pituitary	0.49	1362	2423	3764
PBS - Collimated	PTV	59.21	4948	5141	5249
PBS - Un-collimated	PTV	59.21	4967	5138	5252

Figure 10: Dose statistics for PTV and multiple OARs showing region of interest (ROI) volume, dose to 99% of volume (D99), average dose to volume and dose to 1% of the volume (D1) for collimated and un-collimated PBS plans.

4. Discussion

In this study, we quantified the variation in lateral penumbra as a function of depth, air gap, and range shifter thickness for the PBS mode of proton therapy delivery using the Raystation TPS. The results of this study demonstrated that air gap, depth, and range shifter thickness affect the reduction in the lateral penumbra that can be achieved through aperture collimation.

The reduction in lateral penumbra through the use of an aperture diminished with depth. This was primarily due to increased proton scatter as beam spots traversed the medium. At increased depths, penumbra broadening of collimated beams along field edges due to scattering became similar to the lateral penumbra of un-collimated beams. For this reason, application of an aperture to PBS fields may not be beneficial for deep-seated tumors such as prostate or other abdominal treatment sites. The reduction of lateral penumbra with collimation was negligible (at less than 1 mm) at large depths greater than approximately 20 cm.

We found that for varying depth, airgap and range shifter thickness the RS-MC dose algorithm calculated the lateral penumbra accurately. In particular, for the collimated fields across multiple depths and range shifter thicknesses, RS-MC matched film measurements of lateral penumbra within +/- 1 mm. Previous studies have also demonstrated good agreement between RS-MC and measurements of un-collimated fields (Sorriaux et al., 2017, Saini et al., 2017). Saini et al. validated RS-MC against film measurements in a heterogeneous environment using an Alderson–Rando phantom and found that 6 out of 7 lateral dose profile planes had gamma of greater than 90% using 3%/ 3mm gamma index criteria (Saini et al., 2017). Similarly, Sorriaux et al. found a 95.9% (2%/2mm gamma index criteria) agreement between RS-MC and measurements made with an ion chamber array in a heterogeneous phantom (Sorriaux et al., 2017).

We have also presented a treatment plan generated in Raystation using a patient CT in which un-collimated and collimated PBS beams were optimized and the penumbra across the target volume was analyzed. Baumer et al. has also carried out a similar study using Raystation in which a collimated PBS treatment plan was compared against a uniform scanning plan for the irradiation of an orbit (Baumer et al., 2018). Comparisons of the order of range shifter and aperture and the impact on lateral penumbra were also studied by Baumer et al. Our study differs with Baumer et al. in that we have presented the difference in penumbra with and without aperture collimation across multiple planning parameters. Furthermore, we have derived an analytical formula to predict the lateral penumbra based on depth of target and air gap. Our analytical formula can be used by clinicians prior to planning to decide whether aperture collimation would be valuable for patients who are to receive PBS treatments.

Our analytical formula had the following limitations. First, it was derived in homogeneous media and did not consider heterogeneities found, for example, in the case of an actual patient. This limitation could cause a discrepancy based on differing scatter properties between homogeneous and heterogeneous media. Second, the formula was derived for single beams impinging on a rectangular target. Although this approximation is common in routine proton therapy quality assurance, patients often receive multiple beams impinging on rounded surfaces. As a test of the robustness of our model against these specific limitations, we selected a clinical patient example in which three fields targeted a tumor volume located in the brain of a heterogeneous patient CT. Even with these potential limitations, the penumbra values predicted by Equation 1 agreed well with the TPS-calculated penumbra of the clinical patient example (to within 0.5 mm). Finally, the analytical formula presented in this study was derived using native spot sigma values ranging from 3.2 mm to 7.3 mm. Therefore, this formula may not be valid for proton therapy systems with spot sizes drastically different than that used in this work. Future studies may investigate the effects of adding additional terms to the analytical penumbra model that consider heterogeneities within the patient as well as varying PBS spot sizes.

5. Conclusions

In conclusion, our findings indicate that apertures can measurably sharpen the lateral penumbra of PBS fields using an IBA Proteus Plus proton beam delivery system. The lateral penumbra of collimated PBS beams varied as a function of depth, airgap and range shifter thickness. Our results demonstrated that the use of apertures for PBS treatments is most beneficial for shallow targets while maintaining small air gaps. At approximately 20 cm depth, the benefit of using an aperture became negligible with a collimated penumbra reduction less than 1 mm. In addition, we found that the RS-MC dose engine calculated lateral penumbra with sufficient accuracy for clinical use. PBS penumbra reduction through aperture collimation was also demonstrated on a clinical CT scan for a brain case and the corresponding DVH and dose statistics for the target and affected OARs were presented. Finally, an analytic equation which can predict lateral penumbra reduction between collimated and un-collimated PBS treatments as a function of target depth and airgap was introduced. This analytic equation was able to predict the penumbra reduction within 0.5 mm when compared to the TPS-calculated data for an example brain tumor case.

Acknowledgments

The authors would like to thank Avril O'Ryan-Blair for helping to design the treatment plans used in this study.

References

BAUMER, C., GEISMAR, D., KOSKA, B., KRAMER, P. H., LAMBERT, J., LEMKE, M., PLAUDE, S., PSCHICHHOLZ, L., QAMHIYEH, S., SCHIEMANN, A., TIMMERMANN, B. & VERMEREN, X. 2017. Comprehensive clinical commissioning and validation of the RayStation treatment planning system for proton therapy with active scanning and passive treatment techniques. *Phys Med,* 43**,** 15-24.

BAUMER, C., JANSON, M., TIMMERMANN, B. & WULFF, J. 2018. Collimated proton pencil-beam scanning for superficial targets: impact of the order of range shifter and aperture. *Phys Med Biol,* 63**,** 085020.

CHARLWOOD, F. C., AITKENHEAD, A. H. & MACKAY, R. I. 2016. A Monte Carlo study on the collimation of pencil beam scanning proton therapy beams. *Med Phys,* 43**,** 1462-72.

GOTTSCHALK, B. 2011. Multileaf collimators, air gap, lateral penumbra, and range compensation in proton radiotherapy. *Med Phys,* 38**,** i-ii.

HONG, L., GOITEIN, M., BUCCIOLINI, M., COMISKEY, R., GOTTSCHALK, B., ROSENTHAL, S., SERAGO, C. & URIE, M. 1996. A pencil beam algorithm for proton dose calculations. *Phys Med Biol,* 41**,** 1305-30.

LABORATORIES, R. 2017. RayStation 6 User Manual.

LIU, H. & CHANG, J. Y. 2011. Proton therapy in clinical practice. *Chin J Cancer,* 30**,** 315-26.

PERL, J., SHIN, J., SCHUMANN, J., FADDEGON, B. & PAGANETTI, H. 2012. TOPAS: an innovative proton Monte Carlo platform for research and clinical applications. *Med Phys,* 39**,** 6818-37.

RANA, S., ZEIDAN, O., RAMIREZ, E., RAINS, M., GAO, J. & ZHENG, Y. 2013. Measurements of lateral penumbra for uniform scanning proton beams under various beam delivery conditions and comparison to the XiO treatment planning system. *Med Phys,* 40**,** 091708.

SAFAI, S., BORTFELD, T. & ENGELSMAN, M. 2008. Comparison between the lateral penumbra of a collimated double-scattered beam and uncollimated scanning beam in proton radiotherapy. *Phys Med Biol,* 53**,** 1729-50.

SAINI, J., CAO, N., BOWEN, S. R., HERRERA, M., NICEWONGER, D., WONG, T. & BLOCH, C. 2016. Clinical Commissioning of a Pencil Beam Scanning Treatment Planning System for Proton Therapy. *International Journal of Particle Therapy,* 3**,** 51-60.

SAINI, J., MAES, D., EGAN, A., BOWEN, S. R., ST JAMES, S., JANSON, M., WONG, T. & BLOCH, C. 2017. Dosimetric evaluation of a commercial proton spot scanning Monte-Carlo dose algorithm: comparisons against measurements and simulations. *Phys Med Biol,* 62**,** 7659-7681.

SORRIAUX, J., TESTA, M., PAGANETTI, H., ORBAN DE XIVRY, J., LEE, J. A., TRANEUS, E., SOURIS, K., VYNCKIER, S. & STERPIN, E. 2017. Experimental assessment of proton dose calculation accuracy in inhomogeneous media. *Phys Med,* 38**,** 10-15.

TITT, U., MIRKOVIC, D., SAWAKUCHI, G. O., PERLES, L. A., NEWHAUSER, W. D., TADDEI, P. J. & MOHAN, R. 2010. Adjustment of the lateral and longitudinal size of scanned proton beam spots using a pre-absorber to optimize penumbrae and delivery efficiency. *Phys Med Biol,* 55**,** 7097-106.

URIE, M. M., SISTERSON, J. M., KOEHLER, A. M., GOITEIN, M. & ZOESMAN, J. 1986. Proton beam penumbra: effects of separation between patient and beam modifying devices. *Med Phys,* 13**,** 734-41.

WINTERHALTER, C., LOMAX, A. J., OXLEY, D., WEBER, D. C. & SAFAI, S. 2017. A comprehensive study of lateral fall-off (penumbra) optimisation for pencil beam scanning (PBS) proton therapy. *Phys Med Biol*.